Dynamics of a quantum phase transition with decoherence: Quantum Ising chain in a static spin environment

Lukasz Cincio, Jacek Dziarmaga, Jakub Meisner, and Marek M. Rams
Institute of Physics and Centre for Complex Systems Research, Jagiellonian University, Reymonta 4, 30-059 Kraków, Poland
(Received 11 December 2008; published 23 March 2009)

We consider a linear quench from the paramagnetic to ferromagnetic phase in the quantum Ising chain interacting with a static spin environment. Both decoherence from the environment and nonadiabaticity of the evolution near a critical point excite the system from the final ferromagnetic ground state. For weak decoherence and relatively fast quenches the excitation energy, proportional to the number of kinks in the final state, decays like an inverse square root of a quench time, but slow transitions or strong decoherence makes it decay in a much slower logarithmic way. We also find that fidelity between the final ferromagnetic ground state and a final state after a quench decays exponentially with a size of a chain, with a decay rate proportional to average density of excited kinks and a proportionality factor evolving from 1.3 for weak decoherence and fast quenches to approximately 1 for slow transitions or strong decoherence. Simultaneously, correlations between kinks randomly distributed along the chain evolve from a near-crystalline antibunching to a Poissonian distribution of kinks in a number of isolated Anderson localization centers randomly scattered along the chain.

DOI: 10.1103/PhysRevB.79.094421 PACS number(s): 75.10.Pq, 03.65.−w, 64.60.−i, 73.43.Nq

I. INTRODUCTION

Phase transition is a fundamental change in the state of a system when one of its parameters passes through the critical point. In a second-order phase transition, the fundamental change is continuous and the critical point is characterized by divergences in the correlation length and in the relaxation time. This critical slowing down implies that no matter how slowly a system is driven through the transition, its evolution cannot be adiabatic close to the critical point. As a result, ordering of the state after the transition is not perfect: it is a mosaic of ordered domains whose finite size $\hat{\xi}$ depends on the rate of the transition. This scenario was first described in the cosmological context by Kibble[1] who appealed to relativistic causality to set the size of the domains. The dynamical mechanism relevant for second-order phase transitions was proposed by Zurek.[2] It is based on the universality of critical slowing down and leads to a prediction that average size $\hat{\xi}$ of the ordered domains scales with the transition time τ_Q as

$$\hat{\xi} \simeq \tau_Q^{\nu/(z\nu+1)}, \tag{1}$$

where ν and z are critical exponents. The Kibble-Zurek mechanism (KZM) for second-order thermodynamic phase transitions was confirmed by numerical simulations of the time-dependent Ginzburg-Landau model[3] and successfully tested by experiments in liquid crystals,[4] superfluid helium 3,[5] both high-T_c (Ref. 6) and low-T_c (Ref. 7) superconductors, and even in nonequilibrium systems.[8] With the exception of superfluid ^{4}He—where the early detection of copious defect formation[9] was subsequently attributed to vorticity inadvertently introduced by stirring,[10] and the situation remains unclear—experimental results are consistent with KZM, although more experimental work is clearly needed to allow for more stringent experimental tests of KZM. Quite recently, a new experiment was reported in Ref. 11 where they observe, for the first time, spontaneous appearance of vorticity during Bose-Einstein condensation (BEC) driven by evaporative cooling, confirming KZM predictions in Ref. 12.

The Kibble-Zurek mechanism is thus a universal theory of the dynamics of second-order phase transitions whose applications range from the low-temperature BEC to the ultrahigh-temperature transitions in the grand unified theories of high energy physics. However, the zero-temperature quantum limit remained unexplored until very recently and quantum phase transitions are in many respects qualitatively different from transitions at finite temperature. Most importantly time evolution is unitary, so there is no damping and there are no thermal fluctuations that initiate symmetry breaking in KZM. The recent progress on dynamical quantum phase transitions is mostly theoretical—see Refs. 13–27 and, for an example of a disordered quantum system, Ref. 28—but there is already one significant exception: the experiment in Ref. 29 on a transition from paramagnetic to ferromagnetic phase in a dipolar BEC. Generic outcome of that experiment is a mosaic of finite-size ferromagnetic domains, whose origin was attributed to the Kibble-Zurek mechanism. This explanation is further supported by theory in Ref. 21.

A majority of theoretical work was devoted to the prototypical exactly solvable quantum Ising chain[15,16,19,20,26,27,30]

$$H_S = -\sum_{n=1}^{N} [g\sigma_n^x + \sigma_n^z\sigma_{n+1}^z] \tag{2}$$

driven by a linear quench

$$g(t) = -\frac{t}{\tau_Q} \tag{3}$$

from $g=\infty$ to $g=0$, i.e., across the quantum phase transition from paramagnet to ferromagnet at $g_c=1$. Since the system is gapless at g_c, when $\tau_Q \gg 1$ the evolution becomes nonadiabatic at

$$\hat{g} - g_c \simeq \tau_Q^{1/(z\nu+1)} \tag{4}$$

(see Ref. 15). The freezeout at $\hat{g}$ is the closer to g_c the slower is the transition. The Ising critical exponents $\nu=1$ and $z=1$ determine an average size of ferromagnetic domains at $g=0$ proportional to the correlation length at $\hat{g}$,

$$\hat{\xi} \simeq \tau_Q^{1/2}, \tag{5}$$

or final density of kinks (domain walls) at $g=0$,

$$d \simeq \hat{\xi}^{-1} \simeq \tau_Q^{-1/2}, \tag{6}$$

which is proportional to excitation energy density. Other properties, such as spin-spin correlation functions[19,20] or entropy of entanglement between a block of consecutive spins and the rest of the chain,[20] were analyzed in some detail and they all turned out to be determined by $\hat{\xi}$.

While the quench in isolated system (2) seems to be well analyzed, relatively little is still known about dynamical transitions in open quantum systems subject to interaction with environment. Significant progress was made in Ref. 30 in a "global" case when interaction between the system S with Hamiltonian (2) and its environment E is described by $V=R(\Sigma_n \sigma_n^x)$, where R is a Hermitian operator of the environment. This global model is solvable thanks to its translational invariance, and its solutions indicate that decoherence is increasing density of excited kinks as compared to an isolated system. A local model, with system (2) coupled to an *Ohmic* heat bath, was analyzed in Ref. 31 distinguishing between different regimes of parameters where defect production is dominated by either KZM or external heating. In this paper, we propose a quite realistic, but still solvable, model of local zero-temperature decoherence from a *static* environment. Its solution predicts dramatic increase in the density d of excited kinks as compared to an isolated system with d decaying as only a logarithmic function of τ_Q.

Motivation for this study is twofold. It comes from both condensed matter physics, where it is virtually impossible to isolate a system from its environment, and adiabatic quantum computation, where a system is initially prepared in a simple ground state of a simple initial Hamiltonian H_0 and then it is driven adiabatically to a final Hamiltonian H_1 whose nontrivial ground state is the desired solution of a complex computational problem. The computation is complicated by a quantum critical point somewhere on the way from H_0 to H_1 which can make the adiabaticity problematic, but see Refs. 26 and 27 for methods on how to circumvent this problem. Ising chain (2) is a toy model of adiabatic quantum computer with the final (trivial) ferromagnetic ground state at $g=0$ playing the role of the desired "nontrivial" ground state. When the "computer" is isolated from environment, then Eq. (6) implies that the minimal "computation time" τ_Q required to keep the evolution adiabatic or, equivalently, to make $\hat{\xi} \gg N$ is

$$\tau_Q^{\text{isolated}} \simeq N^2. \tag{7}$$

The "isolated" computation problem is polynomial in N. In contrast, in our model of decoherence similar argument predicts

$$\tau_Q^{\text{open}} \simeq e^{\sqrt{N}}, \tag{8}$$

which is nonpolynomial in N.

II. ISING CHAIN IN STATIC SPIN BATH

In this paper we couple Ising chain (2) to an environment E of M spins through the interaction

$$V = -\sum_{n=1}^{N}\sum_{m=1}^{M} \sigma_n^x V_{nm} \tau_m^x. \tag{9}$$

Here τ_m's are Pauli matrices of environmental spins. The spins are static, with $H_E=0$, and the total Hamiltonian is just $H=H_S+V$.

Initially at $t \to -\infty$ the system is in the ground state $|0_{g\to\infty}\rangle$ of pure Ising chain (2) with all spins polarized along x. This assumption is self-consistent in our open system because large initial energy gap of $2g$ makes the influence of the static environment so negligible that the initial states of S and E can be assumed uncorrelated: $\rho_{S+E}=\rho_S \otimes \rho_E$ with $\rho_S = |0_{g\to\infty}\rangle\langle 0_{g\to\infty}|$ and the environment is initially in a pure state,

$$\sum_{s_1,\ldots,s_M=-1,+1} c_{s_1,\ldots,s_M} |s_1\rangle \ldots |s_M\rangle. \tag{10}$$

Here $\tau_m^x|s_m\rangle = s_m|s_m\rangle$.

After evolution for time Δt reduced density matrix of the system $\rho_S = \mathrm{Tr}_E\, \rho_{S+E}$ becomes

$$\rho_S(\Delta t) = \sum_{\vec{s}} |c_{\vec{s}}|^2 U(\Delta t,\vec{s})|0_\infty\rangle\langle 0_\infty|U^\dagger(\Delta t,\vec{s}) \equiv \overline{U(\Delta t,\vec{s})|0_\infty\rangle\langle 0_\infty|U^\dagger(\Delta t,\vec{s})}. \tag{11}$$

Here $\vec{s}=(s_1,\ldots,s_M)$,

$$U(\Delta t,\vec{s}) = \mathcal{T}\exp\left[-i\int_0^{\Delta t} dt' H(t',\vec{s})\right], \tag{12}$$

and

$$H(t,\vec{s}) = -\sum_{n=1}^{N} \{[g(t)+\Gamma_n]\sigma_n^x + \sigma_n^z\sigma_{n+1}^z\}, \tag{13}$$

with random magnetic fields of the static environment

$$\Gamma_n = \sum_{m=1}^{M} V_{nm} s_m. \tag{14}$$

The overline in Eq. (11) is an average over $\vec{s}$ with probability distribution $|c_{\vec{s}}|^2$, but it can also be interpreted as an average over random "disorder" field Γ_n. $\rho_S(\Delta t)$ is an average over states $U(\Delta t,\vec{s})|0_\infty\rangle$ obtained in quenches with different disordered Hamiltonians (13). In this way, our original problem of a quench in open pure Ising model (2) is mapped to an average over quenches in isolated random Ising model (13).

In the following, rather than struggle with the problem in its full generality, we assume that each spin of the environment couples to only one spin of the system or, in other words, each spin of the system has its own *local* environ-

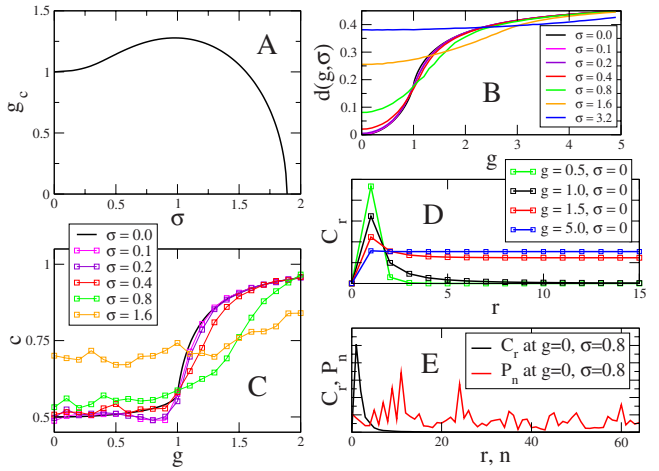

FIG. 1. (Color online) In (A) the critical g_c in Eq. (16) is shown as a function of σ in Eq. (15). In (B) density of kinks in a ground state of the random chain Eq. (13) is shown as a function of g for $N=512$ and different σ's. In (C) we show correlation coefficient c in Eq. (31) as a function of g and σ. When $\sigma<1$, $c\approx 0.5$ in the ferromagnetic phase below $g_c\approx 1$ and $c>0.5$ in the paramagnetic phase above g_c. In (D) we show correlator C_r in Eq. (36) between two kinks in a Cooper pair in the pure Ising chain ($\sigma=0$). C_r is localized below $g_c=1$ and delocalized above. In (E) both C_r and P_n in Eq. (37) are shown in the ferromagnetic phase at $g=0$ and $\sigma=0.8$. Here $N=512$ in both (D) and (E).

ment. Consequently, Γ_m and Γ_n are statistically independent when $m\neq n$. We also assume that each Γ_n has the same Gaussian probability distribution

$$f(\Gamma)=\frac{e^{-\Gamma^2/2\sigma^2}}{\sqrt{2\pi\sigma^2}}, \tag{15}$$

where σ is strength of disorder/decoherence.

Hamiltonian (13) belongs to the universality class of the well-known random Ising chain.[32,33] It has a continuous quantum critical point at g_c when

$$\overline{\ln|g_c+\Gamma|}\equiv\int_{-\infty}^{\infty}d\Gamma f(\Gamma)\ln|g_c+\Gamma|=0. \tag{16}$$

g_c depends on σ as shown in Fig. 1(A). There is no critical point for $\sigma>1.887$ when the disorder is too strong. No matter how weak σ is, renormalization group transformations drive model (13) toward an infinite disorder fixed point with different critical exponents than in the pure Ising chain: the random chain has $\nu=2$ instead of $\nu=1$ and $z\to\infty$ instead of $z=1$.[33] A straightforward application of standard KZ formula (1) gives $\hat{\xi}\simeq 1$, i.e., a domain size that does not depend on the quench time τ_Q. A more careful argument in Ref. 28, going back to the basics of KZM, predicts a logarithmic dependence,

$$\hat{\xi}\simeq\frac{\ln^2[\alpha\tau_Q]}{\ln^2[\ln(\alpha\tau_Q)]}, \tag{17}$$

with a nonuniversal $\alpha\simeq 1$. This equation leads to the estimate in Eq. (8). Since Eq. (17) is based on the universality class alone, it is valid for any model of this class when τ_Q is long enough for the quench to become nonadiabatic, close enough to g_c to be affected by disorder. Estimate (17) was confirmed by numerics in the model of Ref. 28, where it was also found that for weak disorder and relatively fast τ_Q one recovers Eqs. (5) and (6) as in pure model (2).

In present effective model (13), it is simple to estimate how slow a quench needs to be for Eqs. (5) and (6) and, more importantly, Eq. (7) to be not valid. Assuming that influence of Γ_n is negligible, evolution becomes nonadiabatic at a field $\hat{g}$ in Eq. (4). This assumption is not self-consistent when the remaining distance from $\hat{g}$ to g_c, $\hat{g}-g_c\simeq\tau_Q^{-1/2}$, is less than the strength σ of disorder field Γ_n or, equivalently,

$$\tau_Q\sigma^2\gg 1. \tag{18}$$

Thus, no matter how weak the decoherence is, its influence is not negligible when the transition is slow enough: $\tau_Q\gg\sigma^{-2}$. In consequence, there is a maximal number of qubits

$$N\ll\frac{1}{\sigma}, \tag{19}$$

which can be simulated with polynomial efficiency; compare Eqs. (7) and (18).

In Sec. III, we present static properties of random Ising model (13).

III. RANDOM ISING CHAIN

Here we assume for convenience that N is even, and following Refs. 28 and 34, make the Jordan-Wigner transformation $\sigma_n^x=1-2c_n^\dagger c_n$ and $\sigma_n^z=-(c_n+c_n^\dagger)\Pi_{m<n}(1-2c_m^\dagger c_m)$ introducing spinless fermionic operators c_n. Hamiltonian (13) becomes $H=P^+H^+P^++P^-H^-P^-$ where $P^\pm=\frac{1}{2}[1\pm\Pi_{n=1}^N(1-2c_n^\dagger c_n)]$ are projectors on subspaces with even (+) and odd (−) numbers of c quasiparticles and

$$H^\pm=\sum_{n=1}^{N}\left(g_nc_n^\dagger c_n-c_n^\dagger c_{n+1}-c_{n+1}c_n-\frac{g_n}{2}\right)+\text{h.c.} \tag{20}$$

are quadratic Hamiltonians. Here

$$g_n=g+\Gamma_n \tag{21}$$

for short. The c_n's in H^- satisfy periodic boundary conditions $c_{N+1}=c_1$, but the c_n's in H^+ must obey $c_{N+1}=-c_1$: what we call "antiperiodic" boundary conditions.

The parity of the number of c quasiparticles is a good quantum number, and the ground state has even parity for any value of g. Assuming that the quench begins in the ground state we can confine to the subspace of even parity. In this subspace the quadratic H^+ is diagonalized by a Bogoliubov transformation $c_n=\Sigma_{m=1}^N(u_{nm}\gamma_m+v_{nm}^*\gamma_m^\dagger)$. The index m numerates (Bogoliubov) eigenmodes of the stationary Bogoliubov–de Gennes equations

$$\omega_m u_{n,m}^\pm=2g_nu_{n,m}^\mp-2u_{n\mp1,m}^\mp, \tag{22}$$

with $\omega_m>0$. Here we define $u_{nm}^\pm\equiv u_{nm}\pm v_{nm}$ and assume the antiperiodic boundary conditions: $u_{N+1,m}^\pm=-u_{1,m}^\pm, u_{0,m}^\pm=-u_{N,m}^\pm$. The eigenstates (u_{nm},v_{nm}), normalized so that $\Sigma_n(|u_{nm}|^2$

$+|v_{nm}|^2)=1$, define quasiparticle operators $\gamma_m=u^*_{nm}c_n+v^*_{nm}c^\dagger_n$. After the Bogoliubov transformation the Hamiltonian becomes $H^+=\Sigma_{m=1}^N\omega_m(\gamma^\dagger_m\gamma_m-\frac{1}{2})$ which is a simple-looking sum of quasiparticles. However, thanks to the projection $P^+H^+P^+$ only states with even numbers of quasiparticles belong to the spectrum of H.

When $g=\sigma=0$ final system Hamiltonian (2) has N degenerate quasiparticles with $\omega=2$. We choose an orthonormal basis,

$$u^{(0)}_{nm}=\frac{1}{2}(\delta_{n+1,m}-\delta_{n,m}), \tag{23}$$

$$v^{(0)}_{nm}=\frac{1}{2}(\delta_{n+1,m}+\delta_{n,m}), \tag{24}$$

antiperiodic in n. These eigenmodes define Bogoliubov quasiparticles $\gamma^{(0)}_m$ which are simply kinks localized at bonds between sites m and $m+1$. The kinks are related to quasiparticles (u_{nm},v_{nm}) at finite (g,Γ) by a Bogoliubov transformation,

$$\gamma_a=U^*_{ba}\gamma^{(0)}_b+V^*_{ba}\gamma^{(0)\dagger}_b, \tag{25}$$

where

$$U_{ba}=\sum_n(u^{(0)*}_{nb}u_{na}+v^{(0)*}_{nb}v_{na}), \tag{26}$$

$$V_{ba}=\sum_n(v^{(0)}_{nb}u_{na}+u^{(0)}_{nb}v_{na}), \tag{27}$$

leading, for example, to a simple expression for average kink density in the ground state $|0_{g,\Gamma}\rangle$ of Hamiltonian (13) as follows:

$$d(g,\sigma)=\frac{1}{N}\overline{\langle 0_{g,\Gamma}|\sum_{m=1}^N\gamma^{(0)\dagger}_m\gamma^{(0)}_m|0_{g,\Gamma}\rangle}=\frac{\mathrm{Tr}\,V^\dagger V}{N}, \tag{28}$$

as shown in Fig. 1(B). It is finite at any $g>0$, both in the ferromagnetic $(g<g_c)$ and paramagnetic phases $(g>g_c)$, but—as we will see—kink-kink correlations are qualitatively different in the two phases.

These correlations can be indirectly probed by average fidelity F between the final ground state $|0\rangle$ of H_S at $g=0$ (state with no kinks $\gamma^{(0)}$) and ground states $|g,\Gamma_n\rangle$ at finite g or σ;

$$|0_{g,\Gamma}\rangle=\mathcal{N}e^{1/2\Sigma^N_{a,b=1}Z_{ab}\gamma^{(0)\dagger}_a\gamma^{(0)\dagger}_b}|0\rangle. \tag{29}$$

Here $Z=V^*(U^*)^{-1}$ and $\mathcal{N}$ is a normalization factor. The average fidelity is

$$F=\overline{\langle 0|0_{g,\Gamma}\rangle\langle 0_{g,\Gamma}|0\rangle}=1/\overline{\left[\sum_{n=0}^{N/2}\frac{1}{(n!)^2}\langle 0|(\hat{Z}^\dagger)^n\hat{Z}^n|0\rangle\right]}$$
$$=\overline{\mathrm{Det}(1+Z^\dagger Z)^{-1/2}}. \tag{30}$$

Here $\hat{Z}\equiv\frac{1}{2}\Sigma_{ab}Z_{ab}\gamma^{(0)\dagger}_a\gamma^{(0)\dagger}_b$ for short.

We found that the fidelity is exponential in N;

$$F(g,\sigma,N)\sim(1-cd)^N, \tag{31}$$

when $F\ll 1$. Here $d(g,\sigma)$ is the density of kinks in Eq. (28) and Fig. 1(B). The coefficient $c(g,\sigma)$ is shown in Fig. 1(C). For weak disorder, when $\sigma\ll 1$, we have $c\approx\frac{1}{2}$ when $g<g_c$, with c increasing toward 1 when $g\gg g_c$ or $\sigma\gg 1$. These two limits can be explained as follows.

When the magnetic fields $g_n=\Gamma_n+g$ in effective Hamiltonian (13) are strong, because either g or σ or both are strong, then in any ground state $|0_{g,\Gamma}\rangle$ all spins are polarized along σ^x. Fidelity to the σ^z ferromagnet is $F=1/2^N$, and density of kinks is $d=1/2$; hence, $F=(1-cd)^N$ with $c=1$. This c is consistent with the data shown in Fig. 1(C) when g or σ is strong.

In the opposite limit of weak magnetic fields $|g_n|=|g+\Gamma_n|\ll 1$, the ground states are

$$|0_{g,\Gamma}\rangle\approx\prod_{n=1}^N\frac{|\uparrow_n\rangle\pm\frac{g_n}{4}|\downarrow_n\rangle}{\sqrt{1+\frac{g_n^2}{16}}}. \tag{32}$$

Their fidelity to the σ^z ferromagnet is

$$F=\prod_{n=1}^N\frac{1}{1+\frac{g_n^2}{16}}\approx\left(1-\frac{1}{2}d\right)^N, \tag{33}$$

when $F\ll 1$. Here $d=\frac{1}{8}\overline{g_n^2}\ll 1$ is small density of kinks and $c=1/2$. This c is consistent with the data in Fig. 1(C) when $\sigma\ll 1$ and $g<g_c\approx 1$.

It is interesting to interpret the widely different values of $\frac{1}{2}\leq c<1$ in terms of a simple Poissonian model where each of N bonds is either excited (with probability d_{exc}) or not excited (with probability $1-d_{\mathrm{exc}}$) *independently* of other bonds. Here d_{exc} is average density of excitations. The fidelity is a probability that none of the N independent bonds is excited

$$F=(1-d_{\mathrm{exc}})^N. \tag{34}$$

Comparing Eqs. (31) and (34) we obtain density of *independent* excitations,

$$d_{\mathrm{exc}}=cd. \tag{35}$$

We can conclude that $c=d_{\mathrm{exc}}/d$ measures correlations between kinks: $c<1$ means bunching, and an eventual $c>1$ would mean antibunching of kinks randomly distributed along the spin chain.

This simple interpretation of c follows from the fact that any ground state $|0_{g,\Gamma}\rangle$ is a Bardeen-Cooper-Schrieffer (BCS) state of kinks $\gamma^{(0)}$; see Eq. (29) where Z_{ab} is a wave function for a (Cooper) pair of kinks. Depending on g and σ, this BCS state can be either a condensate of tightly bound Cooper pairs of kinks (with $c=1/2$) or just a weakly coupled BCS state with pairing (anti-)correlations manifesting as the (anti-)bunching of kinks.

The BCS state is particularly simple at weak magnetic fields $g_n=g+\Gamma_n$ when, crudely speaking, the ground state $|0_{g,\Gamma}\rangle$ in Eq. (32) is approximately the ferromagnet $|\uparrow_1\uparrow_2\ldots\uparrow_N\rangle$ but with occasional spins reversed to $|\downarrow_n\rangle$ by weak magnetic fields $g_n\sigma^x_n$. Each reversed spin is a tightly bound Cooper pair of two kinks sitting on nearest-neighbor

bonds with a relative distance of $r=1$ lattice sites between the two kinks. No wonder that $d_{\rm exc}=d/2$ in this case.

As we could see in Fig. 1(C), the picture with tightly bound Cooper pairs is accurate for weak disorder in the ferromagnetic phase, but with g increasing above g_c the Cooper pairs begin to dissociate into free kinks and antikinks and c increases well above $\frac{1}{2}$. This dissociation can be clearly seen in Fig. 1(D) where we show a correlation function C_r,

$$C_r \sim \sum_m |Z_{m+r,m}|^2, \tag{36}$$

between two kinks making a Cooper pair. Here $Z_{a,b}$ is the un-normalized wave function of a Cooper pair of two kinks in BCS state (29) and r is a relative distance between the two kinks. The C_r shown in Fig. 1(D) is localized when $g<=g_c$ (tight Cooper pairs) and delocalized when $g>g_c$ (dissociated pairs).

A similar C_r is shown in Fig. 1(E) for a finite $\sigma=0.8$ in the ferromagnetic phase at $g=0$. In addition, the same figure shows reduced probability distribution,

$$P_n \sim \sum_m |Z_{m,n}|^2, \tag{37}$$

for a single kink. Unlike in the pure case, this P_n is not uniform and shows Anderson localization.

In the ferromagnetic phase below g_c all kinks are bound into tight Cooper pairs. The small density of Cooper pairs, each of them a tightly bound pair of kink and antikink, does not destroy long-range ferromagnetic order in σ^z. With g increasing above g_c the transition to the paramagnetic phase takes place when the Cooper pairs begin to dissociate into free kinks and antikinks which scramble long-range ferromagnetic correlations.

In the context of adiabatic quantum computation there are two generally accepted measures of how far the final state $\rho_S(0)$ from the desired final ground state $|0\rangle$ is. One is energy of excitation of the final state above the energy of the desired final ground state, and the other is fidelity between the final state and the final ground state. Both quantities are tractable in our model, where the excitation energy is proportional to the number of kinks. We study them in the following Secs. IV and V.

IV. DENSITY OF KINKS AFTER A QUENCH

In our simulations of a quench the system is initially prepared in its ground state at a large initial value of $g \gg 1$, i.e., in a Bogoliubov vacuum state for quasiparticles at an initial $g \gg 1$. As the magnetic field is being turned off to zero across g_c, the state of the system $|\psi(t)\rangle$ is getting excited from its adiabatic ground state. However, in a similar way, as in Refs. 16 and 28, we use the Heisenberg picture where the state remains a vacuum for quasiparticle operators,

$$\tilde{\gamma}_m = u^*_{nm}(t)c_n + v^*_{nm}(t)c^\dagger_n, \tag{38}$$

with the Bogoliubov modes $u_{nm}(t)$ and $v_{nm}(t)$ solving time-dependent Bogoliubov–de Gennes equations

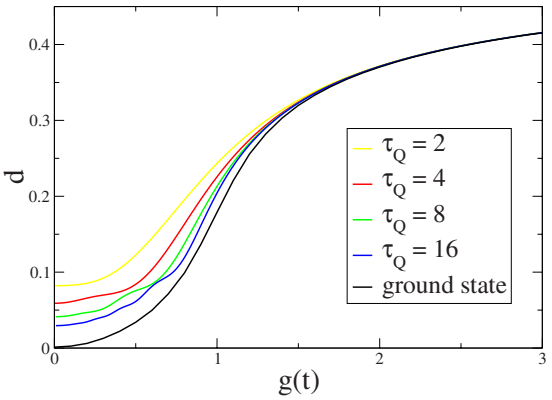

FIG. 2. (Color online) Density of kinks during a quench as a function of $g(t)$. Here each plot is a single realization with $\sigma=0.1$ on a lattice of $N=512$ sites. For the early large g the density follows the density $d(g,\sigma)$ in a ground state $|0_{g,\Gamma}\rangle$, but as the quench is approaching the critical point $g_c \approx 1$ the evolution becomes nonadiabatic and the density gets excited above its ground state level. The slower the quench is, the closer to the critical point the nonadiabatic stage begins and the quench is probing the critical point more closely.

$$i\frac{du^{\pm}_{n,m}}{dt} = 2g_n(t)u^{\mp}_{n,m} - 2u^{\mp}_{n\mp1,m}. \tag{39}$$

Initially each mode is a positive frequency eigenmode of stationary equation (22). Equation (39) was integrated by a split-step method for each realization of Γ_n. Their solutions $u^{\pm}_{nm}(0)$ at the final $g=0$ determine final states $|\psi(0)\rangle$ whose average over disorder gives final density matrix $\rho_s(0) = \overline{|\psi(0)\rangle\langle\psi(0)|}$. For each realization of Γ_n, a final state $|\psi(0)\rangle$ is a vacuum for $\tilde{\gamma}_m$'s which are related to the kinks $\gamma^{(0)}_m$ by transformation (25). Final densities of kinks follow from Eq. (28).

For system Hamiltonian (2) at the final $g=0$ the final excitation energy is simply twice the final number of kinks excited in the desired ferromagnetic ground state. In Fig. 2 we show density of kinks d as a function of $g(t)$. For the early large g the density follows the density $d(g,\sigma)$ in a ground state $|0_{g,\Gamma}\rangle$, which is also shown in Fig. 1(B), but as the quench is approaching the critical point $g_c \approx 1$ the evolution becomes nonadiabatic and the density d is excited above its ground-state level $d(g,\sigma)$. The slower the quench is, the closer to the critical point the nonadiabatic stage begins and the quench is probing the critical point more closely.

The final density of kinks at $g=0$ is shown in Fig. 3(A). For large τ_Q, the density tends to saturate at $d(g=0,\sigma)$, shown in Fig. 1(B), i.e., the density of kinks in the ground state of random Hamiltonian (13). In Fig. 3(B) we show a difference $\delta d = d - d(g=0,\sigma)$ which can be attributed to the nonadiabaticity of the transition described by KZM. If $\delta d = \alpha\tau_Q^w$, then in the log-log plot of Fig. 3(B) we would see a line $\log_{10}\delta d = \log_{10}\alpha + w(\log_{10}\tau_Q)$, but this is not the case when $\tau_Q \gg \sigma^{-2}$ as in Eq. (18). At best we can think of a local slope $w(\tau_Q)$ which can be estimated by fitting to pairs of nearest-neighbor data points. In the legend we give ranges of local slopes w obtained for different σ's (with error bars on

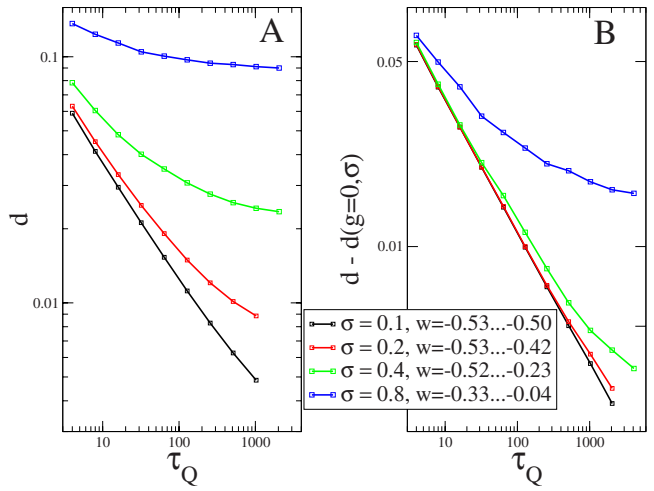

FIG. 3. (Color online) In (A) final density of kinks at $g=0$ is shown as a function of τ_Q on a $N=512$ chain. For large τ_Q the density tends to saturate at the average density of kinks $d_{g=0,\sigma}$ in the ground state of random Hamiltonian (13) shown in Fig. 1(B). In (B) we show difference $\delta d=d-d_{g=0,\sigma}$ which is density of kinks excited above the ground state of the random Hamiltonian at $g=0$. This difference can be attributed to the nonadiabaticity of the transition described by KZM.

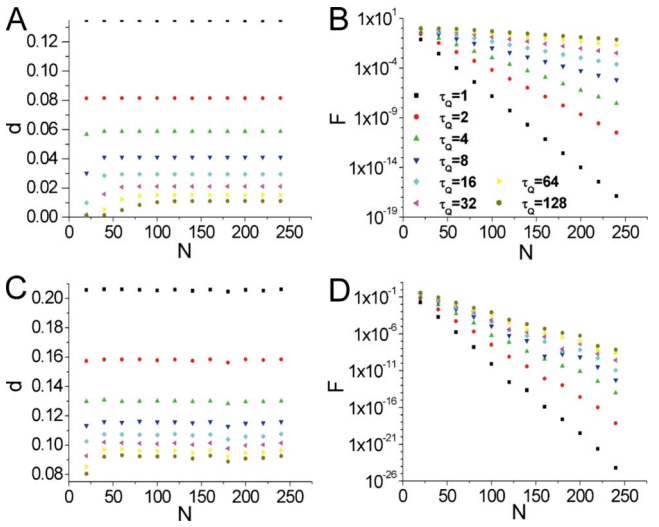

FIG. 4. (Color online) In (A) and (C) final kink density d for different τ_Q as functions of lattice size N for $\sigma=0.1$ (panel A) and $\sigma=0.8$ (panel C). In (B) and (D) fidelity F for $\sigma=0.1$ (panel B) and $\sigma=0.8$ (panel D). With increasing N the density saturates at an asymptotic $d(\tau_Q,\sigma)$ when $N\gg 1/d(\tau_Q,\sigma)$. In the same asymptotic regime the fidelity becomes exponential in N. Here the averages are taken over N_R realizations with $N_R N\geq 2048$.

their last digits). For weak σ and small τ_Q the slope w is close to the $-1/2$ characteristic for pure model (2): fast quenches, when $\tau_Q\ll\sigma^{-2}$, become nonadiabatic far enough from the critical point not to see any effect of weak disorder. At stronger σ or longer τ_Q the local slopes are less steep and for a fixed σ they become less steep with increasing τ_Q. For example, at the strongest $\sigma=0.8$ the local slope falls to a mere $|w|=0.04$ for the longest τ_Q. These observations are consistent with the predicted logarithmic dependence of the dynamical correlation length $\hat{\xi}$ in Eq. (17).

V. FIDELITY AND CORRELATIONS AFTER A QUENCH

In the context of adiabatic quantum computation, it is important to know how close the final state $\rho_S(0)$ to the desired ground state of the final Hamiltonian H_S is. The closeness is measured by fidelity,

$$F=\langle 0|\rho_S(0)|0\rangle=\overline{\langle 0|\psi(0)\rangle\langle\psi(0)|0\rangle}, \tag{40}$$

given by Eq. (30).

Without decoherence, or in a pure Ising chain with $\sigma=0$, the fidelity can be obtained analytically from the exact solution in Refs. 16 and 20. F is a probability that not a single pair of $\gamma^{(0)}$ quasiparticles with opposite quasimomenta $(k,-k)$ is excited after a quench, $F=\Pi_{k>0}(1-p_k)$. Here $p_k\approx\exp(-2\pi\tau_Q k^2)$ when $\tau_Q\gg 1$. When $Nd\gg 1$ we obtain

$$\ln F\approx -\frac{Nd}{2}\frac{\int_0^\infty ds\,\ln[1-e^{-s^2}]}{\int_0^\infty ds e^{-s^2}}\approx -1.3Nd. \tag{41}$$

Here $d=\int_{-\pi}^{\pi}\frac{dk}{2\pi}p_k=1/2\pi\sqrt{2\tau_Q}$. F is exponential in N as in the static case of Eq. (31). Given that $d\ll 1$ for $\tau_Q\gg 1$ we obtain that $c\approx 1.3>1$, implying antibunching of kinks.

The antibunching can also be seen in the state $|\psi(0)\rangle$ after a quench which is a BCS state of kinks in Eq. (29). Figure 6(A) shows a probability distribution P_n for a kink in Eq. (37) and the correlation function C_r between two kinks in a Cooper pair in Eq. (36) after a quench with $\sigma=0$ and $\tau_Q=16$. We have $C_0=0$ because the kinks are fermions, there is a broad maximum in C_r in the range $|r|=20\ldots 40$, and a flat distribution for $|r|>40$ when the Cooper pair is dissociated. If C_r were flat everywhere (except $r=0$), then $c=1$, but the broad maximum means that even when the kinks get close to each other they prefer to keep a safe distance in the range of $20\ldots 40$. This short range repulsion is consistent with the antibunching observed in Eq. (41) where $c=1.3>1$.

The same antibunching can also be seen in the ferromagnetic correlation function after a quench at $g=0$,

$$\langle\sigma_i^z\sigma_{i+R}^z\rangle\simeq\exp(-1.55Rd)\cos(2.95Rd-\varphi), \tag{42}$$

accurate when $1\ll R\ll\sqrt{\tau_Q}\log\tau_Q$ (see Ref. 20). The oscillatory cosine factor means that kinks tend to order into a crystal lattice. This very imperfect crystalline order implies the antibunching seen in $c=1.3>1$. We can conclude that in the state after a quench with $\sigma=0$ there is a similar connection between c, C_r, and ferromagnetic correlations as in the static case.

For quenches with $\sigma>0$ we also find an exponential tail,

$$F(\tau_Q,\sigma)\sim(1-cd)^N, \tag{43}$$

when $F\ll 1$ (compare panels B and D in Fig. 4). Here $d(\tau_Q,\sigma)$ is an asymptotic value of average kink density obtained for a sufficiently large lattice size N such that $Nd(\tau_Q,\sigma)\gg 1$ (see panels A and C in Fig. 4). In contrast, when $N\ll 1/d(\tau_Q,\sigma)$, then a finite gap at $g=g_c$ results in an

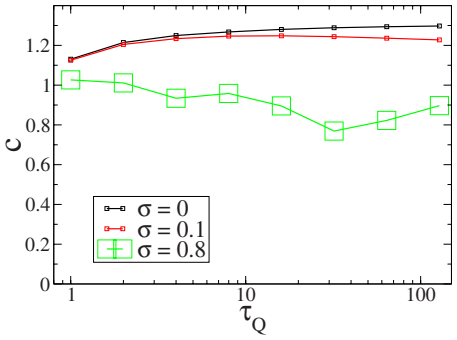

FIG. 5. (Color online) Correlation coefficients c for different τ_Q and σ obtained by linear fits to the exponential tails of fidelity in Figs. 4(B) and 4(D).

adiabatic transition and a final density of kinks which is less than the asymptotic $d(\tau_Q,\sigma)$ for large N.

Fits to the exponential tails of fidelity in Figs. 4(B) and 4(D) give correlation coefficients c for different τ_Q and σ which are shown in Fig. 5. For comparison, we also show in the same figure c at $\sigma=0$ which saturates at $c=1.3$ when $\tau_Q \gg 1$. The results suggest that for a strong σ or large τ_Q, when even a weak σ has strong effect, the correlation coefficient decays toward $c \approx 1$, suggesting random Poissonian trains of kinks and exponential ferromagnetic correlation functions.

This picture is corroborated by typical correlation functions C_r and probability distributions P_n shown in panels B–E of Fig. 6. Here it is clear, especially for the larger $\tau_Q=1024$ (green) or the stronger $\sigma=0.8$ (panels C and E), that a kink gets localized in isolated Anderson localization centers. A close inspection of corresponding C_r's reveals that C_r is localized at r's equal to distances between the localization centers in P_n. There is only one exception from this rule: C_r is negligible when $r \approx 0$ or N because, apparently, a (Cooper) pair of fermionic kinks avoids being trapped in the same localization center. It seems that each kink in a Cooper pair chooses its localization center at random, independently of the other kink, except for avoiding the same localization center. A quantitative proof of this simple picture is provided in Figs. 7(B) and 7(C) where we plot a convolution,

$$PP_r = \sum_{n=1}^{N} P_n P_{n+r}. \tag{44}$$

If the two kinks in a Cooper pair were independent, then this convolution would reconstruct the corresponding C_r's in Figs. 6(B) and 6(C). Comparing panels B and C in the two figures we see that it does, with the expected exceptions when $r \approx 0, N$ and in the case of a fast quench ($\tau_Q=16$) at weak $\sigma=0.1$ [black in Fig. 6(B)]. We can conclude that, with some idealization, for long τ_Q or strong σ, final kinks are distributed as if each kink was choosing at random one of the isolated Anderson localization centers randomly distributed along the chain. This approximate Poissonian model is consistent with the observed $c \approx 1$.

When $\tau_Q \sigma^2 \gg 1$, then the final states at $g=0$ are qualitatively different from the ground state of random Hamiltonian

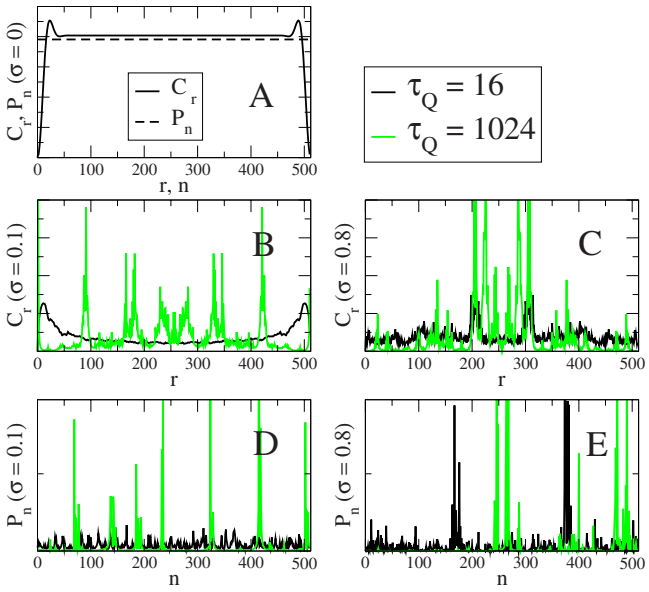

FIG. 6. (Color online) In (A) a correlation function C_r between two kinks in a Cooper pair and probability distribution P_n for a kink on a $N=512$ periodic lattice after a quench with $\sigma=0$ and $\tau_Q=16$. In (B)–(E) we show typical final C_r and P_n after quenches with $\sigma=0.1, 0.8$ and $\tau_Q=16, 1024$. Here all C_r and P_n for a given σ come from the same realization of disorder Γ_n. Both C_r and P_n show Anderson localization. When τ_Q or σ are large, then C_r is localized around those r's which can be identified as distances (modulo periodic boundary conditions) between the localization centers in the corresponding P_n, with the exception of $r \approx 0$ which is avoided because two fermionic kinks do not like to choose the same localization center.

(13) at $g=0$: the (green) fragmented C_r's in Figs. 6(B) and 6(C) are qualitatively different from the (black) C_r in Fig. 1(E) localized around $r=0$. In other words, all kinks in the ground state, of density $d(g=0,\sigma)$, are tightly bound into Cooper pairs which do not destroy ferromagnetic long-range order; while all kinks in a final state, of density d, contribute to exponentially decaying ferromagnetic correlations even though for slow quenches the difference $\delta d = d - d(0,\sigma)$, whose origin can be attributed to nonadiabaticity, is small as compared to $d(0,\sigma)$.

These striking properties of the final states after a quench are inherited from the ground state of the random Hamiltonian (13) just above g_c. Its properties are relevant here because, as we could see in Fig. 2, in a slow quench a state

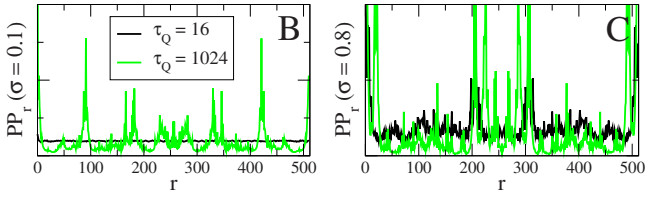

FIG. 7. (Color online) In (B) and (C) convolutions in Eq. (7) corresponding to C_r's in Figs. 6(B) and 6(D) obtained from distributions P_n in Figs. 6(D) and 6(E). Except for $\tau_Q=16$, $\sigma=0.1$ (black in panels B), the convolutions are very close to their corresponding C_r's everywhere apart from r close to 0 (and N).

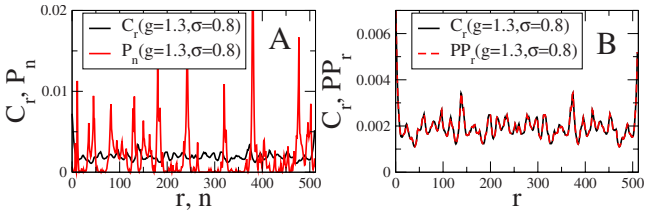

FIG. 8. (Color online) In (A) C_r and P_n in a ground state of random Hamiltonian (13) at $\sigma=0.8$ and $g=1.3$ just above g_c. Here P_n shows similar fragmentation into isolated Anderson localization centers as in the final states after a quench with long τ_Q or large σ in Figs. 6. In (B) we show both the C_r from panel A and a convolution PP_n in Eq. (44) obtained form the P_n in panel A. The two plots are identical except for $r=0$, demonstrating independence of kinks.

$|\psi(t)\rangle$ follows an adiabatic ground state of the random Hamiltonian until a $\hat{g}$ just above g_c when, in accordance with KZM, the evolution becomes nonadiabatic. In Fig. 8, we show some properties of the ground state just above g_c where P_n is fragmented into isolated localization centers, and C_r is identical with PP_r everywhere except $r=0$. Apparently, the following evolution from $\hat{g}$ to $g=0$ does not change this qualitative picture.

VI. CONCLUSION

A static spin environment increases nonadiabaticity of the transition in a dramatic way: density of quasiparticles (kinks) decays no longer as a power of the transition time but in a much slower logarithmic way. This means, in the context of adiabatic quantum computation, that coupling to a static environment may transform a polynomial computational problem into a nonpolynomial one.

Fidelity between a final state after a quench and the desired final ground state decays exponentially with a chain size. The rate of this decay is equal to the density of kinks times a correlation coefficient equal, for fast transitions and weak decoherence, to 1.3 and, for slow transitions or strong decoherence, close to 1. Corresponding kink-kink correlations are, respectively, antibunching in a near-crystalline ordering and a simple Poissonian distribution of kinks in isolated Anderson localization centers randomly distributed along a chain.

ACKNOWLEDGMENTS

We would like to thank Wojciech Zurek for discussions. Work of L.C., J.D., J.M., and M.M.R. was supported in part by Polish government scientific funds (2008–2011) as research Projects No. N N202 175935, No. N N202 079135, No. N 202 059 31/3195, and No. N N202 174335, respectively, and in part by Marie Curie Actions Transfer of Knowledge project COCOS (Contract No. MTKD-CT-2004-517186).

[1] T. W. B. Kibble, J. Phys. A **9**, 1387 (1976); Phys. Rep. **67**, 183 (1980).
[2] W. H. Zurek, Nature (London) **317**, 505 (1985); Acta Phys. Pol. B **24**, 1301 (1993); Phys. Rep. **276**, 177 (1996).
[3] P. Laguna and W. H. Zurek, Phys. Rev. Lett. **78**, 2519 (1997); Phys. Rev. D **58**, 085021 (1998); A. Yates and W. H. Zurek, Phys. Rev. Lett. **80**, 5477 (1998); G. J. Stephens, E. A. Calzetta, B. L. Hu, and S. A. Ramsey, Phys. Rev. D **59**, 045009 (1999); N. D. Antunes, L. M. A. Bettencourt, and W. H. Zurek, Phys. Rev. Lett. **82**, 2824 (1999); J. Dziarmaga, P. Laguna, and W. H. Zurek, *ibid.* **82**, 4749 (1999); M. B. Hindmarsh and A. Rajantie, *ibid.* **85**, 4660 (2000); G. J. Stephens, L. M. A. Bettencourt, and W. H. Zurek, *ibid.* **88**, 137004 (2002).
[4] I. L. Chuang, R. Durrer, N. Turok, and B. Yurke, Science **251**, 1336 (1991); M. J. Bowick, L. Chandar, E. A. Schiff, and A. M. Srivastava, *ibid.* **263**, 943 (1994).
[5] V. M. H. Ruutu, V. B. Eltsov, A. J. Gill, T. W. B. Kibble, M. Krusius, Yu. G. Makhlin, B. Plaçais, G. E. Volovik, and W. Xu, Nature (London) **382**, 334 (1996); C. Bäuerle, Yu. M. Bunkov, S. N. Fisher, H. Godfrin, G. R. Pickett, *ibid.* **382**, 332 (1996).
[6] R. Carmi, E. Polturak, and G. Koren, Phys. Rev. Lett. **84**, 4966 (2000); A. Maniv, E. Polturak, and G. Koren, *ibid.* **91**, 197001 (2003).
[7] R. Monaco, J. Mygind, and R. J. Rivers, Phys. Rev. Lett. **89**, 080603 (2002); Phys. Rev. B **67**, 104506 (2003); R. Monaco, J. Mygind, M. Aaroe, R. J. Rivers, and V. P. Koshelets, Phys. Rev. Lett. **96**, 180604 (2006).
[8] S. Ducci, P. L. Ramazza, W. González-Viñas, and F. T. Arecchi, Phys. Rev. Lett. **83**, 5210 (1999); S. Casado, W. González-Viñas, H. Mancini, and S. Boccaletti, Phys. Rev. E **63**, 057301 (2001); S. Casado, W. González-Viñas, S. Boccaletti, P. L. Ramazza, and H. Mancini, Eur. Phys. J. Spec. Top. **146**, 87 (2007).
[9] P. C. Hendry, N. S. Lawson, R. A. M. Lee, P. V. E. McClintock, and C. D. H. Williams, Nature (London) **368**, 315 (1994).
[10] M. E. Dodd, P. C. Hendry, N. S. Lawson, P. V. E. McClintock, and C. D. H. Williams, Phys. Rev. Lett. **81**, 3703 (1998).
[11] D. R. Scherer, C. N. Weiler, T. W. Neely, and B. P. Anderson, Phys. Rev. Lett. **98**, 110402 (2007).
[12] J. R. Anglin and W. H. Zurek, Phys. Rev. Lett. **83**, 1707 (1999).
[13] J. Dziarmaga, A. Smerzi, W. H. Zurek, and A. R. Bishop, Phys. Rev. Lett. **88**, 167001 (2002).
[14] B. Damski, Phys. Rev. Lett. **95**, 035701 (2005).
[15] W. H. Zurek, U. Dorner, and P. Zoller, Phys. Rev. Lett. **95**, 105701 (2005).
[16] J. Dziarmaga, Phys. Rev. Lett. **95**, 245701 (2005).
[17] A. Polkovnikov, Phys. Rev. B **72**, 161201(R) (2005).
[18] F. M. Cucchietti, B. Damski, J. Dziarmaga, and W. H. Zurek, Phys. Rev. A **75**, 023603 (2007).
[19] R. W. Cherng and L. S. Levitov, Phys. Rev. A **73**, 043614 (2006).
[20] L. Cincio, J. Dziarmaga, M. M. Rams, and W. H. Zurek, Phys. Rev. A **75**, 052321 (2007).
[21] B. Damski and W. H. Zurek, Phys. Rev. Lett. **99**, 130402 (2007); M. Uhlmann, R. Schützhold, and U. R. Fischer, *ibid.* **99**,

120407 (2007).
[22] V. Mukherjee, A. Dutta, and D. Sen, Phys. Rev. B **77**, 214427 (2008); D. Sen, K. Sengupta, and S. Mondal, Phys. Rev. Lett. **101**, 016806 (2008).
[23] T. Caneva, R. Fazio, and G. E. Santoro, Phys. Rev. B **78**, 104426 (2008).
[24] K. Sengupta, D. Sen, and S. Mondal, Phys. Rev. Lett. **100**, 077204 (2008).
[25] J. Dziarmaga, J. Meisner, and W. H. Zurek, Phys. Rev. Lett. **101**, 115701 (2008).
[26] G. Schaller, Phys. Rev. A **78**, 032328 (2008).
[27] R. Barankov and A. Polkovnikov, Phys. Rev. Lett. **101**, 076801 (2008).
[28] J. Dziarmaga, Phys. Rev. B **74**, 064416 (2006); T. Caneva, R. Fazio, and G. E. Santoro, *ibid.* **76**, 144427 (2007).
[29] L. E. Sadler, J. M. Higbie, S. R. Leslie, M. Vengalattore, and D. M. Stamper-Kurn, Nature (London) **443**, 312 (2006).
[30] S. Mostame, G. Schaller, and R. Schützhold, Phys. Rev. A **76**, 030304(R) (2007); A. Fubini, G. Falci, and A. Osterloh, New J. Phys. **9**, 134 (2007).
[31] D. Patane, A. Silva, L. Amico, R. Fazio, and G. E. Santoro, Phys. Rev. Lett. **101**, 175701 (2008).
[32] R. Shankar and G. Murthy, Phys. Rev. B **36**, 536 (1987); B. M. McCoy and T. T. Wu, Phys. Rev. **176**, 631 (1968); **188**, 982 (1969); R. B. Griffiths, Phys. Rev. Lett. **23**, 17 (1969); B. M. McCoy, *ibid.* **23**, 383 (1969); Phys. Rev. **188**, 1014 (1969).
[33] D. S. Fisher, Phys. Rev. B **51**, 6411 (1995).
[34] E. Lieb, T. Schultz, and D. Mattis, Ann. Phys. (N.Y.) **16**, 407 (1961); S. Katsura, Phys. Rev. **127**, 1508 (1962).